International Journal of Engineering Inventions
e-ISSN: 2278-7461, p-ISSN: 2319-6491
Volume 15, Issue 9 [September 2026] PP: 169-182

An Experimental Study of Ambient Temperature Effect on 30-kW Turbine Generator Using Biogas in a Swine Farm

Hsing-Sheng Chai[a] *, Cheng-Yu Tsai[a], Tsung-Han Lee[b], Chen-Kai Luo[b], Tai-Chuan Ge[b] and Chiun-Hsun Chen [b]

[a]*Department of Air Transport Industry, Aletheia University, New Taipei City 251306, Taiwan, R.O.C.*
[b]*Department of Mechanical Engineering, National Chiao-Tung University, 1001 University Road, Hsinchu, 30056, Taiwan, R.O.C.*

ABSTRACT
This study performed experiments on a 30-kW micro-gas turbine engine (CR30) to generate electricity from biogas on a swine farm. Different concentrations of methane in desulfurized biogas were examined to investigate the ambient temperature and workload effects on the performance of the CR30. Theoretical calculations were initially conducted using Brayton cycle assumptions together with actual component efficiencies and experimental data as inputs. The results showed that the calculated generator power output and thermal efficiency were 31.54 kW and 25.62%, respectively. The ambient temperature effects on the performance of the CR30 were subsequently investigated under various workloads (15-30 kW). When the ambient temperature increased from 21.8 to 31.4 °C, the net power output and thermal efficiency decreased by 9.6 and 2.9%, respectively. However, the CH4 concentrations (48-64%) in the biogas did not affect the net power output as long as the CR30 did not reach its maximum operational speed (~96,000 rpm). Finally, comparisons with other research using a CR30 with different fuels, such as propane (21-30 °C) and pure methane (15 °C), were provided. These comparisons showed greater net power outputs with biogas but lower thermal efficiencies compared to propane and pure methane. Comparing with propane, the maximum discrepancies of net power output and thermal efficiency were 1.02 kW and 3.8%, respectively.
KEYWORDS: *biogas generation, gas turbine engine, and ambient temperature.*

Date of Submission: 12-09-2026 Date of acceptance: 24-09-2026

I. INTRODUCTION

Global warming has increased because of increasing concentrations of greenhouse gases, such as carbon dioxide, chlorofluorocarbons, nitrous oxide, water vapor, and methane, in the atmosphere. The major contributor is carbon dioxide resulting from the combustion of fossil fuels that have supplied power to mankind since the Industrial Revolution. To resolve energy shortages and reduce carbon dioxide emissions, the development of renewable energy has attracted significant attention. Recent research has focused on power generation from gas turbines that use biogas—a type of bioenergy. Methane is a flammable fuel, and a biogas containing methane can be used as a renewable fuel.

The predominant livestock in Taiwan is swine, and their manure creates a significant impact on the environment. This study examines the use of manure to produce biogas for electric power generation while simultaneously alleviating the pressure of manure on environmental protection issues.

Tsai and Lin[1] surveyed bioenergy from livestock manure management in Taiwan and calculated the quantity of methane generated from livestock by using practical characteristics of total swine from farm scales of over 1000 pigs. The results from assessing approximately 4.3 million pigs showed that methane emissions could be reduced by 21.5 Gg/year and total generated electricity could be increased by 7.2×107 kWh per year, equivalent to an electricity charge savings of US$ 7.2×106 and a carbon dioxide mitigation of 500 Gg per year.

Su et al.[2] assembled a greenhouse gas production database from anaerobic livestock wastewater treatment processes in Taiwan and compared the livestock wastewater treatment system presented by the IPCC with those used in Taiwan. An analysis of GHG samples from in situ anaerobic wastewater treatment systems of pig and dairy farms revealed average emissions of 0.768 and 4.898/kgCH_4, 0.714 and 4.200/kgCO_2, and 0.002 and 0.011/kgN_2O per pig per year, respectively, during three temperature periods (average temperatures of <20, 20–25, and >25 °C).

Basrawi et al.[3] investigated the effect of the inlet air temperature on the performance of a micro gas turbine (MGT) with cogeneration system (CGS) arrangement. They used a MGT-CGS model to test system performance on the basis of experimental results and simulation under different ambient temperature conditions in a cold region. The results showed a decrease in MGT electricity production with increased temperature, but the ratios of exhaust heat to mass flow rate and exhaust heat recovery to mass flow rate increased during the summer peak.

De Sa et al.[4] employed specific turbines (SGT 94.2 and SGT 94.3) in experiments at the DEWA Power Station. Their results showed that high ambient temperatures led to low thermal efficiency and useful power output. The gas turbines lost 0.1% thermal efficiency and 1.47MW of Gross Power Output with each temperature increase of 1 Kelvin. The gas turbine inlet temperature was a limiting factor because of the turbine blade metallurgy and the reduced mass flow of air at high temperature.

Erdem et al.[5] considered two gas turbine models and seven climate regions in Turkey. Using average regional monthly temperature data for both models, they determined that annual electricity production would decrease and fuel consumption would increase compared to standard design conditions. The results showed that when temperatures rose above the standard ambient temperatures by 15 degrees Celsius, electricity production loss rates would vary between 1.67 and 7.22%. When inlet temperatures decreased to 10 degrees, electricity generation would increase from 0.27 to 10.28%.

Sheng et al.[6] investigated the effect of ambient temperature on the performance of gas turbine under the assumption that electricity production, fuel consumption, and plant incomes were affected by temperature. They found that power decreased due to reductions in the air mass flow rate and efficiency decreased because the compressor required more power to operate in higher temperatures.

Bakalis and Stamatis[7] used a hybrid system consisting of a solid oxide fuel cell and a Capstone micro gas turbine system. The system was simulated in an Aspen PlusTM process simulator and analyzed for exergy destruction, i.e., the amount of work obtainable when the system is in an unbalanced state. The results showed that the SOFC stack and burner accounted for higher exergy destruction rates. Exhaust gases account for a significant amount of exergy loss, and increased SOFC stack temperatures lead to increased system exergy efficiency.

Vidal et al.[8] structured a simple model for a Capstone 30 kW micro gas turbine and carried out simulations at high ambient temperatures under maximum rated power outputs to analyze the corresponding performance. Their results showed that the net output power decreased with increasing ambient temperature. The net power decreased by 5.1% as the ambient temperature was raised from 24.4 to 28.9 °C, and electrical efficiency suffered a 2% reduction.

Homam Nikpey Somehsaraei et al.[9] investigated the fuel flexibility and performance of micro gas turbine (100 kW). Their results showed that electrical efficiency and recuperator effectiveness decreased with an increase of power output; however, these will decrease with ambient temperature. The methane content methane (45, 60, and 70%) in the biogas changed the fuel properties; the power output and electrical efficiency of the biogas decreased with the decreasing percentages of methane in the biogas. Because of this, the biogas fuel mass flow rate was greater than that of natural gas.

This study uses treated biogas to operate a micro gas turbine engine (CR30) manufactured by Capstone. The performance of the MGT is analyzed with a Brayton cycle and an isentropic efficiency of components for obtaining temperatures that are not measured. The ambient temperature is a crucial parameter for a turbine engine. Thus, the performance of this micro gas turbine engine is investigated at various ambient temperatures.

II. EXPERIMENTAL SECTION

The experimental layout and biogas pretreatment system is shown in Figure 1. The micro gas turbine engine is a CR30 unit manufactured by Capstone. The thermal mass flow meter (TBT-FT004) is manufactured by Taiwan Bally Technology. The flow meter is installed in front of the combustor inlet to measure the biogas flow rates. The measurement range of the flow sensor is 5-2830 L/min, with an accuracy of approximately ±3% of the measured value. The compositions of the waste gases are measured with a gas analyzer (IR-208) that is manufactured by IR INFRARED INDUSTRIES and set at the engine outlet. This analyzer measures the concentrations of oxygen, carbon monoxide, carbon dioxide, and methane. The measurement accuracy is approximately ±0.25% of full scale with a resolution of 0.1 ppm. The biogas first passes through a cyclone and filter to remove liquid water and impurities that can damage the engine. The front compressor then treats the biogas by increasing its pressure and temperature by reducing its volume to the corresponding pressure of the combustor. The compressor outlet temperature is approximately 40 °C and the biogas pressure is 5 kgf/cm2. The biogas then passes through a freeze dryer to remove water vapor to enhance power output; the biogas temperature is thus reduced to 36 °C. Finally, the biogas is stored in an 800-liter pressurized tank (5.6 kgf/cm2) for subsequent mixing with air and ignition in the combustor. The compositions of the waste gases are measured with a gas analyzer (IR-208) that is set at the engine outlet, and the waste gas temperature is measured with a K-type thermocouple.

Figure 2 shows the schematic procedure of a micro gas turbine engine. The major components include a centrifugal compressor, a radial turbine, an annular combustor, and an annular recuperator. The compressor, turbine, and generator are mounted on a shaft that is supported by patented air bearings and can spin at up to 96,000 rpm. The turbine provides power to the drive compressor and generator.

The air initially passes through an air filter to remove impurities and then absorbs heat from the cooling fins of the generator to protect the generator from heating damage. The air is then accelerated and pressured by the compressor to attain the pressure limitations in the combustion chamber, where the compressed air will pass through the recuperator to enhance its temperature to reduce fuel consumption and increase thermal efficiency. The heat exchanger fluid is comprised of exhaust gases that are expelled from the turbine engine outlet. The air is then mixed with treated biogas and drawn into the combustor for igniting. Finally, the hot gases drive the turbine blades to generate electricity.

Figure 3 shows the system stability of the CR30. The data points are obtained after users increase the rated power output to analyze engine stability and ensure the timing for recording the data. The net power output is obtained from a power meter that records the current after it is consumed by the compressor and freeze dryer. Therefore, the recorded power outputs are lower than the actual rated power output generated by the MGT. The MGT system approaches stability after two minutes of operation, which is set as the standard consult time for recording data in this study.

The following calculations include thermal efficiency and will be used in the analyses of the following experiments.

The thermal efficiency is defined as the ratio of the actual power generation to the energy input; its formula is as follows:

$$Thermal\ \ Efficiency = \frac{Actual\ \ Power\ \ Generation}{Energy\ \ Input} \tag{1}$$

The actual power generation of this study is the net power output of the turbine generator. The energy input is calculated from the lower heating value (LHV) of methane, which is 50,020 kJ/kg. It is expressed as

$$Energy\ \ Input = \dot{m}_{CH_4} \times LHV\ \ of\ \ CH_4 \tag{2}$$

where $\dot{m}_{CH_4}$ is the methane mass flow rate in biogas, which is calculated by

$$\dot{m}_{CH_4} = \dot{V}_{biogas} \times \rho_{biogas@1atm,25°C} \times mf_{CH_4@5atm} \tag{3}$$

where $\dot{V}_{biogas}$ is the measured biogas volumetric flow rate, $\rho_{biogas@1atm,25°C}$ is the biogas density under normal conditions, and $mf_{CH_4@5atm}$ is the mass fraction of CH_4 in the biogas at five atmospheric pressure.

The theoretical calculation of performance is calculated with a Brayton cycle and the rated efficiency of the component.[10] The temperature and pressure points are indicated in Figure 2. The exit temperatures of components cannot be directly measured by instruments due to Aerospace Industrial Development Corporation (AIDC) restrictions, hence, the isentropic efficiencies noted above are applied for estimating the actual temperatures of the components.

η_c is the isentropic efficiency of the compressor, and η_T is the isentropic efficiency of the turbine. This can be expressed as

$$\eta_C = \frac{W_{C,isen}}{W_C} \tag{4}$$

$$\eta_T = \frac{W_T}{W_{T,isen}} \tag{5}$$

where $W_{C,isen}$ is the isentropic work required by the compressor, $W_{T,isen}$ is the isentropic work output from the turbine, W_C is the realistic work input from the compressor, and W_T is the realistic work output from the turbine. Equations 4 and 5 are applied to calculate the actual outlet temperature of the compressor and the actual inlet temperature of the turbine, respectively.

$$W_C = \frac{\dot{m}_{air} \times C_{p,air} \times (T_2 - T_1)}{\eta_{mech}} \tag{6}$$

$$W_T = \dot{m}_{gas} \times C_{p,gas} \times (T_4 - T_5) \times \eta_{mech} \tag{7}$$

$$W_{C,isen} = \dot{m}_{air} \times C_{p,air} \times (T_{2s} - T_1) \tag{8}$$

$$W_{T,isen} = \dot{m}_{gas} \times C_{p,gas} \times (T_{4s} - T_{5s}) \tag{9}$$

where η_{mech} is the mechanical efficiency.
W_{net} is the net output of the turbine minus the compressor and can be expressed as

$$W_{net} = W_T - W_C \tag{10}$$

The hot gas mass flow rate that drives the turbine blades can be expressed as

$$\dot{m}_{gas} = \dot{m}_{air} + \dot{m}_{biogas} \tag{11}$$

where $\dot{m}_{air}$ is the air mass flow rate and $\dot{m}_{biogas}$ is the biogas mass flow rate. The air mass flow rate is measured with Capstone remote monitoring software and the biogas mass flow rate is obtained from the following:

$$\dot{m}_{biogas} = \dot{V}_{biogas} \times \rho_{biogas@1atm,25°C} \tag{12}$$

The specific heat capacity mixing air with biogas is expressed as

$$C_{p,gas} = \frac{C_{p,air} \times \dot{m}_{air} + C_{p,biogas} \times \dot{m}_{biogas}}{\dot{m}_{air} + \dot{m}_{biogas}} \tag{13}$$

In an ideal gas reversible adiabatic process, the isentropic compressor outlet temperature and the turbine inlet temperature can be expressed as follows:

$$T_{2s} = T_1 \times (\frac{P_2}{P_1})^{k-1/k} \tag{14}$$

$$T_{5s} = \frac{T_{4s}}{(\frac{P_4}{P_5})^{k-1/k}} \tag{15}$$

where k is a gas constant number, $\frac{P_2}{P_1}$ is expressed as r_p and called a pressure ratio. Due to the drop in pressure, $\frac{P_4}{P_5}$ is expressed as follows:

$$\frac{P_4}{P_5} = \frac{P_2}{P_1} \times \Delta P_{recuperator} \times \Delta P_{combustor} \tag{16}$$

where $\Delta P_{recuperator}$ and $\Delta P_{combustor}$ represent the drop in pressure of the recuperator and combustor, respectively.

The heat exchanger effectiveness η_{HE} is calculated by

$$\eta_{HE} = \frac{(\dot{m} \times C_P)_{air} \times (T_3 - T_2)}{(\dot{m} \times C_P)_{air} \times (T_5 - T_2)} = \frac{(\dot{m} \times C_P)_{gas} \times (T_5 - T_6)}{(\dot{m} \times C_P)_{air} \times (T_5 - T_2)} \tag{17}$$

The combustion efficiency is expressed as

$$\eta_{comb} = \frac{(\dot{m}_{gas} \times C_{p,gas} \times T_4) - (\dot{m}_{air} \times C_{p,air} \times T_{3a} + \dot{m}_{biogas} \times C_{p,biogas} \times T_{biogas})}{\dot{m}_{CH_4} \times LHV_{CH_4}} \tag{18}$$

The calculated heat exchanger outlet temperature (gas side) is

$$T_6 = T_5 - \frac{\dot{m}_{air} \times C_{p,air} (T_5 - T_2) \times \eta_{HE}}{\dot{m}_{gas} \times C_{p,gas}} \tag{19}$$

The isentropic thermal efficiency is the ratio of the power output to the ideal heat input:

$$\eta_{isen} = \frac{(W_{T,isen} - W_{C,isen})}{Q_{ideal}} \tag{20}$$

$$Q_{ideal} = (\dot{m}_{gas} \times C_{p,gas} \times T_{4s}) - (\dot{m}_{air} \times C_{p,air} \times T_{3s} + \dot{m}_{biogas} \times C_{p,biogas} \times T_{biogas}) \tag{21}$$

The calculated thermal efficiency is the ratio of the calculated power output of a device to the calculated heat input. Its formula can be expressed as

$$\eta_{th,cal} = \frac{(W_{net} \times \eta_{generator}) - W_{consumption}}{Q_{th,cal}} \tag{22}$$

$$Q_{th,cal} = (\dot{m}_{gas} \times C_{p,gas} \times T_4) - (\dot{m}_{air} \times C_{p,air} \times T_3 + \dot{m}_{biogas} \times C_{p,biogas} \times T_{biogas}) \tag{23}$$

where $Q_{th,cal}$ is the calculated heat input, $\eta_{generator}$ is the generator efficiency, $(W_T - W_C) \times \eta_{generator}$ is the generator power output, and $W_{consumption}$ is the internal consumption of the MGT.

The actual thermal efficiency ($\eta_{th,actual}$) is the ratio of the calculated output of a device to the measured heat input; its formula can be expressed as

$$\eta_{th,actual} = \frac{(W_T - W_C) \times \eta_{generator} - W_{consumption}}{Q_{th,actual}} \tag{24}$$

$$Q_{th,actual} = \dot{m}_{CH_4} \times LHV_{CH_4} \tag{25}$$

where $Q_{th,actual}$ is actual heat input.

III. RESULTS AND DISCUSSION

The experimental study is carried out with 30kW micro-gas turbine (MGT) in a swine farm in Taichung. It is one of products of Capstone so no refit can be allowed. Note that the turbine outlet temperature is always fixed at 594 ºC under any operation, assigned by Capstone. The effect of ambient temperature on engine performance is investigated with an aid of theoretical analyses. The performance of micro gas turbine (MGT) is calculated by Brayton cycle and the ambient temperature effect on MGT is investigated.

3.1 Theoretical Calculation of Performance for Micro-Gas Turbine Engine

A case of rated power output of 25kW (corresponding a maximum engine rotational speed 96,000rpm) at ambient temperature 31.4 ºC is given to demonstrate the theoretical analysis. The system is assumed as in steady state, and C_ps' do not change with temperature. Then, it follows air standard cycle, internally reversible one, and the fluid is ideal gas. The locations of temperatures and mass flow rates are marked in Figure 2, and the input data are shown in Table 1. The air, methane and biogas mass flow rates and compressor inlet and turbine outlet temperatures are measured by sensors. The other parameters are obtained from AIDC and reference [7].

As to the pressure ratio and isentropic efficiencies of compressor and turbine, they are found by using the compressor and turbine performance maps [7] under the specified corrected mass flow rate and engine speed ratio. The corrected mass flow rate is expressed as:

$$\dot{m}_{correct} = \dot{m}_{air} \times \sqrt{\frac{T_{ambient}}{T_{s\tan dard}}} \times \sqrt{\frac{P_{s\tan dard}}{P_{ambient}}} \tag{26}$$

where $\dot{m}_{correct}$ is corrected mass flow rate, $\dot{m}_{air}$ air mass flow rate, $T_{ambient}$ ambient temperature, $T_{s\tan dard}$ temperature at standard condition, $P_{s\tan dard}$ pressure at standard condition and $P_{ambient}$ ambient pressure.

The engine speed ratio is defined as

$$N = \frac{N_{present}}{N_{\max}} \tag{25}$$

where $N_{present}$ is present engine speed and $N_{\max}$ maximum engine speed of turbine engine in the experiment. Table 2 shows the results of theoretical calculation.

Figure 4 shows the actual and theoretical generator power outputs, they are almost parallel and the difference is around 5 kW. The discrepancy is attributed to that the combustor is assumed as adiabatic in calculation and the pressure drop, occurred in air passage (piping loss), does not consider as well. As expected, the theoretical powers are higher than experimental ones.

3.2 Power Generation by Gas Turbine Engine

The biogas used in this research is supplied from the anaerobic tank made of red plastic bag. It is treated in advance with H_2S removal system due to the high concentration of H_2S (~5000 ppm) that will corrode the engine severely. By this process, the concentration of H_2S in biogas is decreased to 50 ppm. The contents of desulfurized biogas at each ambient temperature are shown in Table 4.1. In real situation, the biogas should not contain any O_2 after anaerobic process, however, it shows a lot of air in biogas, indicating that there are leakages from atmosphere to storage tank and biological desulphurization process. Moreover, the concentrations of biogas are 64, 51.7, 60 and 47.8% at ambient temperature 21.8, 23.5, 29.5 and 31.4°C, respectively. It indicates that the content of CH_4 in the treated biogas changes day by day because such gas is not produced by an industrial process. In addition, the water vapor in biogas cannot be not removed completely even it passes through the dryer.

Figure 5 shows the net power output v.s. rated power output from 15~30kW under four different ambient temperatures. It shows that both are almost coincident until the engine speed reaches 96000 rpm in 27, 28, 25, 24 kW at 21.8, 23.5, 29.5 and 31.4 °C, respectively. After that, the maximum net power output apparently is influenced by the ambient temperature. The discrepancy between the rated and net power output becomes greater as the ambient temperature is higher. However, when MGT achieves maximum engine rotational speed (96,000 rpm), the net power outputs of 26, 27, 28 and 30 kW rated powers at 23.5 °C are higher than those at 21.8 °C. The reason is that the CH_4 concentration of biogas is 51.7% at 23.5 °C, whereas it is 64% at 21.8 °C. When the CH_4 concentration becomes lower, MGT will automatically increases the open ratio of fuel valve (Woodward Valve) to supply more biogas for maintaining the combustion. So does the air supply. Since the engine speeds are almost maintained as constant (~96000rpm) at these rated powers, the enhanced total mass flow rate increases the net power output.

Figure 6 shows the CH_4 mass flow rate at different ambient temperatures between 15 and 24 kW of rated power output, where the corresponding the engine speed does not run at the maximum value. It indicates that the CH_4 mass flow rate is enhanced as the ambient temperature increases, but it seems not to relate with CH_4 concentration in biogas. The reason can be explain as follows. As the ambient temperature rises, the recuperator heat recovery and total mass flow rate decrease, as mentioned above. The discrepancy of recuperator heat recovery and total mass flow rate lead the fuel valve to open larger to supply more energy to increase the engine speed for attaining the fixed turbine outlet temperature and required rated power output at higher ambient temperature. Thus, it also results in the engine speed rotating faster to reach 96000 rpm at higher ambient temperature.

Figure 7 shows the thermal efficiency increases with the decrease of ambient temperature at each rated power output. In the normal operation condition between 15 and 25kW of rated power output, the thermal efficiency increases with the rated power at ambient temperatures of 23.5, 29.5 and 31.4℃. It is because MGT operates at partial loads with inlet guide vanes partially open. The gas turbine has higher internal friction losses. On the other hand, it is keep more or less constant (21.4~22.4%) at 21.8℃, whose biogas possesses 64% of CH_4. From the Technical Reference of Capstone, CR30 can achieve the best performance corresponding to thermal efficiency 26±2% by using natural gas (~100% of CH_4) at ambient temperature 15℃. It seems to indicate that the low-cost treated biogas (low H_2S) from livestock's manure can fully utilize the gas turbine to generate power.

3.3 Comparisons with Other Researches

The comparisons with other experiments are made for analyzing the effect on CR30 by using different types of fuel. The fuel used by Adrian Vidal et al.[8] is propane, whereas the fuel used in present study is biogas, whose constituents are varied often.

Figure 8 shows the comparison of thermal efficiency. It can be seen that our thermal efficiency is lower than that of Adrian Vidal et al.[8] It is because the biogas has a poorer quality in combustion, and it has to input more biogas for maintaining the net power output. Thus, the thermal efficiency is decreased. Moreover, with the ambient temperature increasing, our thermal efficiency decreases rapidly. At 31.4 ºC of ambient temperature, the CH_4 concentration of biogas is 48%, which is lower than others. According to the Somehsaraei's study,[9] it confirms that the lower CH_4 concentration of biogas, the smaller thermal efficiency.

The net power output and electric efficiency are in a linear relationship obviously, thus, they can be predicted for consultation by using least square method. Figures 9 and 10 show the results by using the least square fit technique. The equations are expressed as following:

- Net Power Output

This study:

$$P = 33.165 - 0.291T \quad , \quad R^2 = 0.9548 \quad , \quad 21.8^\circ C \le T \le 32^\circ C$$

Adrian Vidal et al.[8]:

$$P = 33.121 - 0.3122T \quad , \quad R^2 = 0.985 \quad , \quad 24.4^\circ C \le T \le 28.9^\circ C$$

- Electric Efficiency

This study:

$$E = 0.2789 - 0.0027T \quad , \quad R^2 = 0.9316 \quad , \quad 21.8^\circ C \le T \le 32^\circ C$$

Adrian Vidal et al.[8]:

$$E = 0.2645 - 0.00135T \quad , \quad R^2 = 0.9781 \quad , \quad 24.4^\circ C \le T \le 28.9^\circ C$$

Our goodness of fit (R^2) is a litter worse than that of Adrian Vidal et al. [8] due to the fewer experimental data points. However, they select more accurate data by rejecting deviated ones. The other reason is that the concentration of CH_4 in biogas is variable often, thus, the measured data possesses the larger variations, causing the smaller goodness of fit (R^2).

IV. CONCLUSIONS

Based on the results of this study, the following conclusions can be asserted.

1. The theoretical calculation is based on Brayton cycle and air standard cycle. The results showed that the theoretical thermal efficiency is 25.62 %, generator power output is 31.54 kW in 25 kW of rated power output at 31.4 °C.
2. Net and rated power outputs are almost coincident until the engine speed reaches 96000 rpm. After that, the maximum net power output decreases with increase of ambient temperature.
3. The thermal efficiency decreases with the increase of ambient temperature at each rated power output. When the ambient temperature increases from 21.8 to 31.4°C, the thermal efficiency decreases 2.8%.
4. The CH_4 mass flow rate is enhanced as the ambient temperature increases, but it does not to relate with CH_4 concentration in biogas.
5. The MGT using biogas has greater net power output than one using propane, whereas the thermal efficiency using biogas is lower.

V. FIGURES

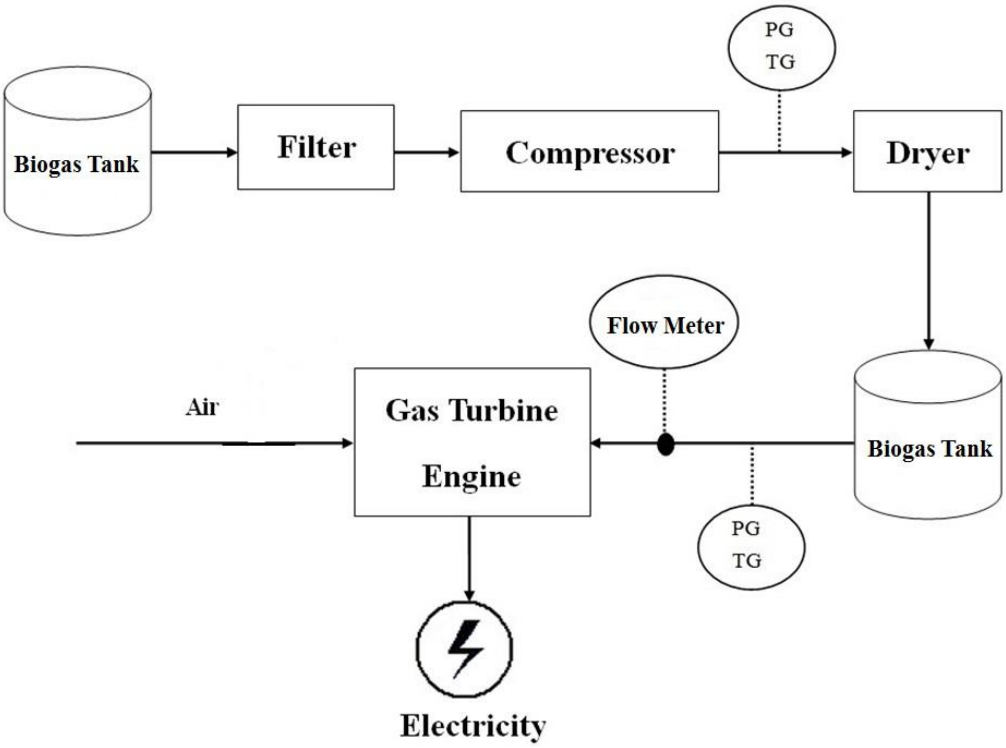

Figure 1 Experiment Layout & Biogas Pretreatment System

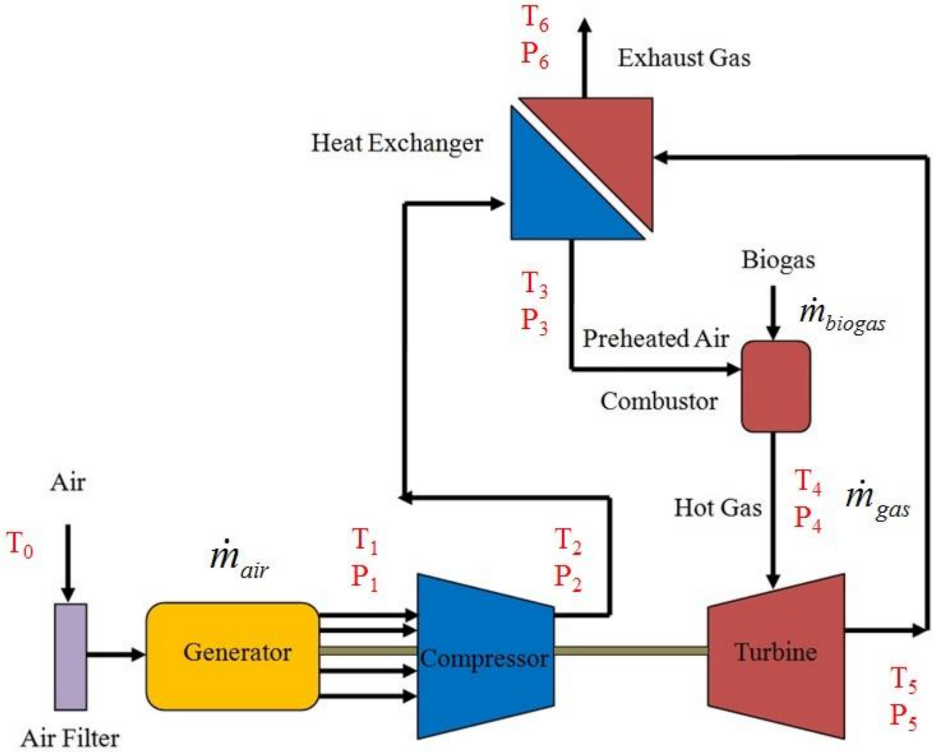

Figure 2 Schematic Procedure of Micro-Gas Turbine Engine

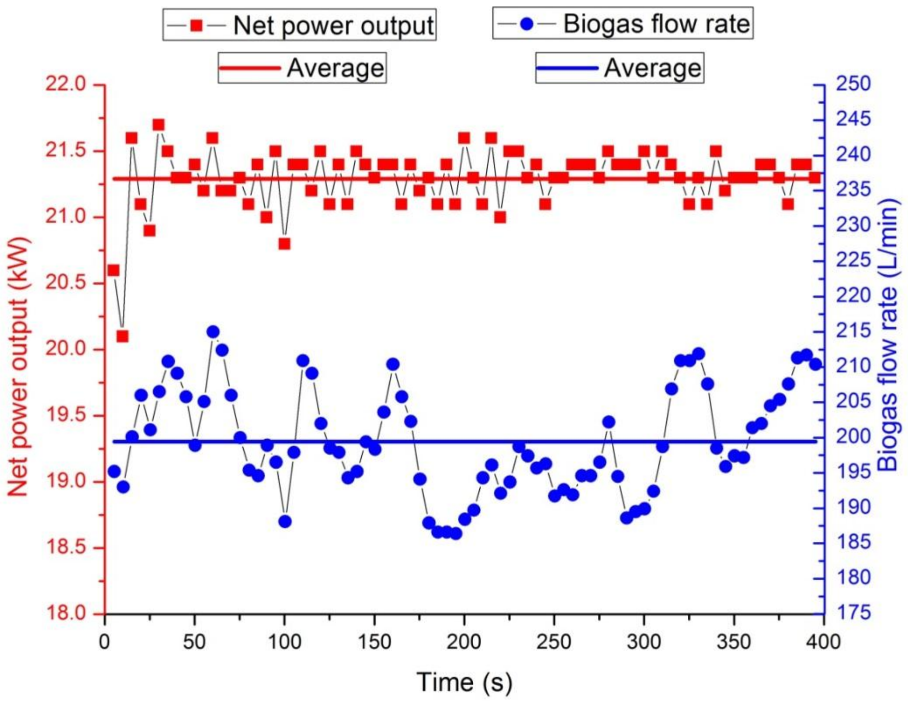

Figure 3 CR30 System Stability in 22 kW

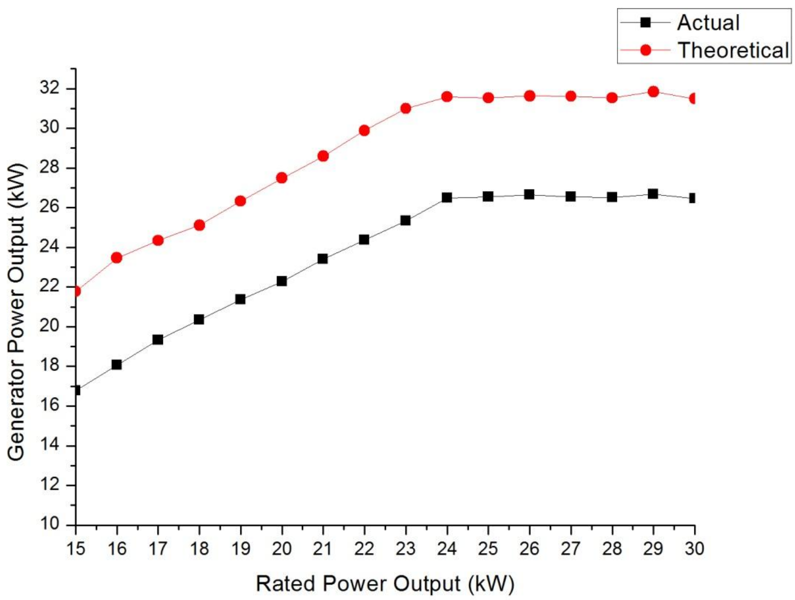

Figure 4 Generator Power Output V.S. Rated Power Output

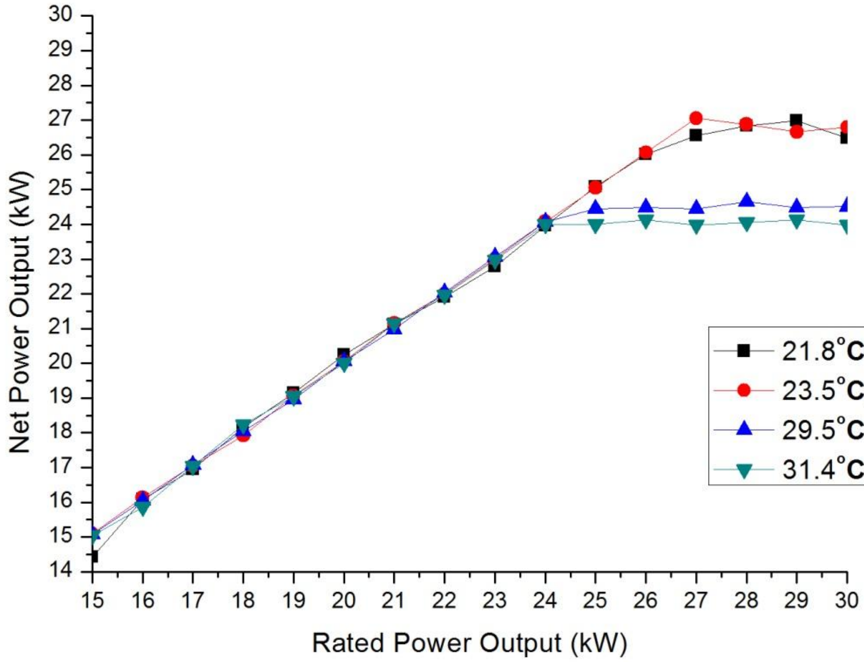

Figure 5 Net Power Output v.s. Rated Power Output

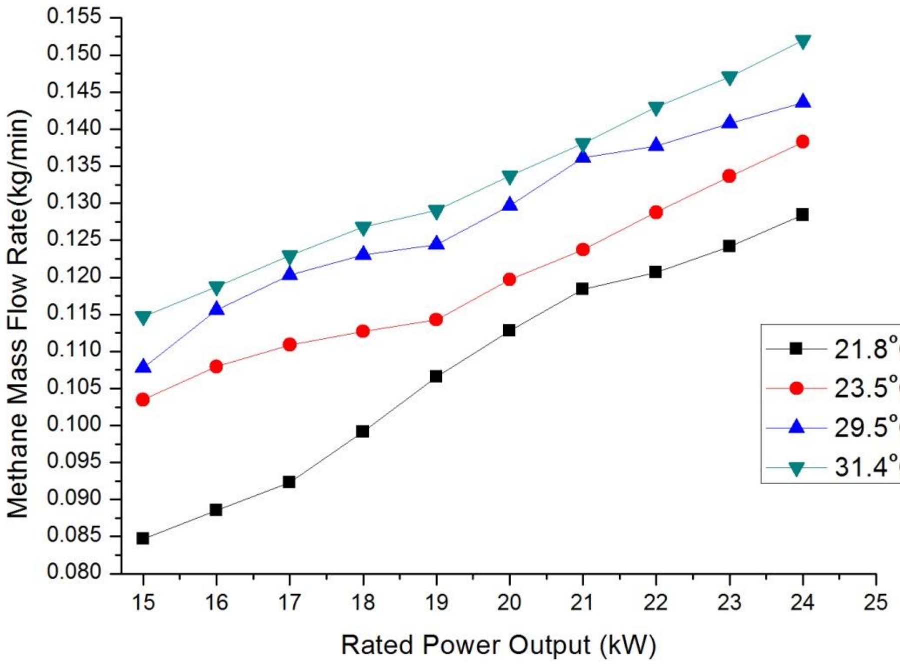

Figure 6 Methane Mass Flow Rate at Different Ambient Temperature

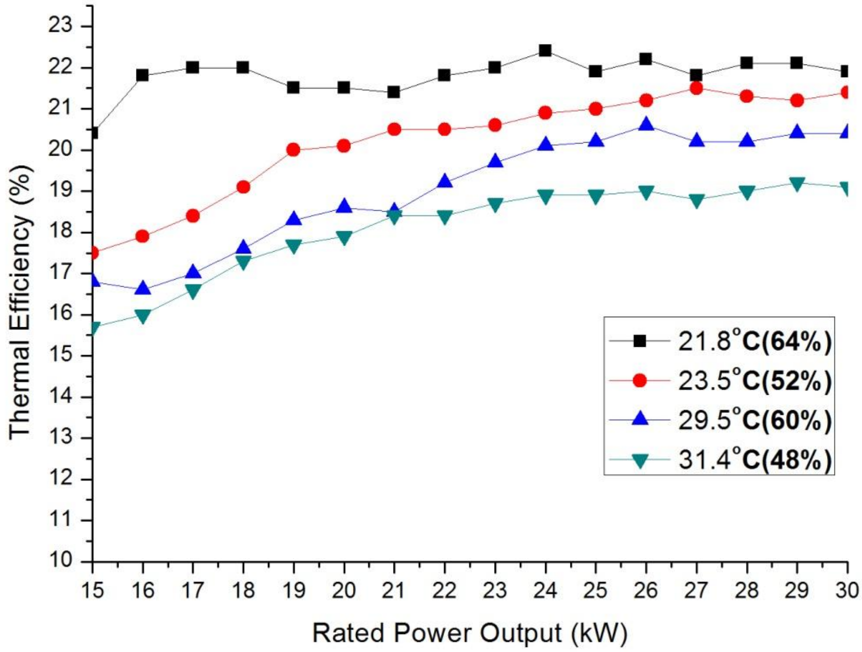

Figure 7 Thermal Efficiency v.s. Rated Power Output

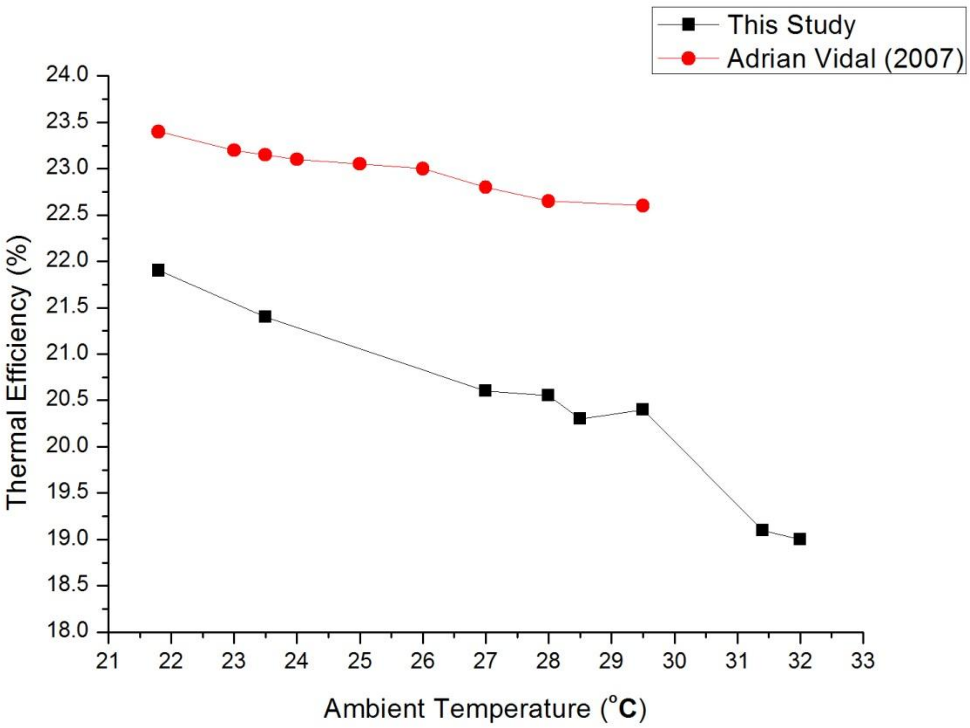

Figure 8 Comparison of Thermal Efficiency

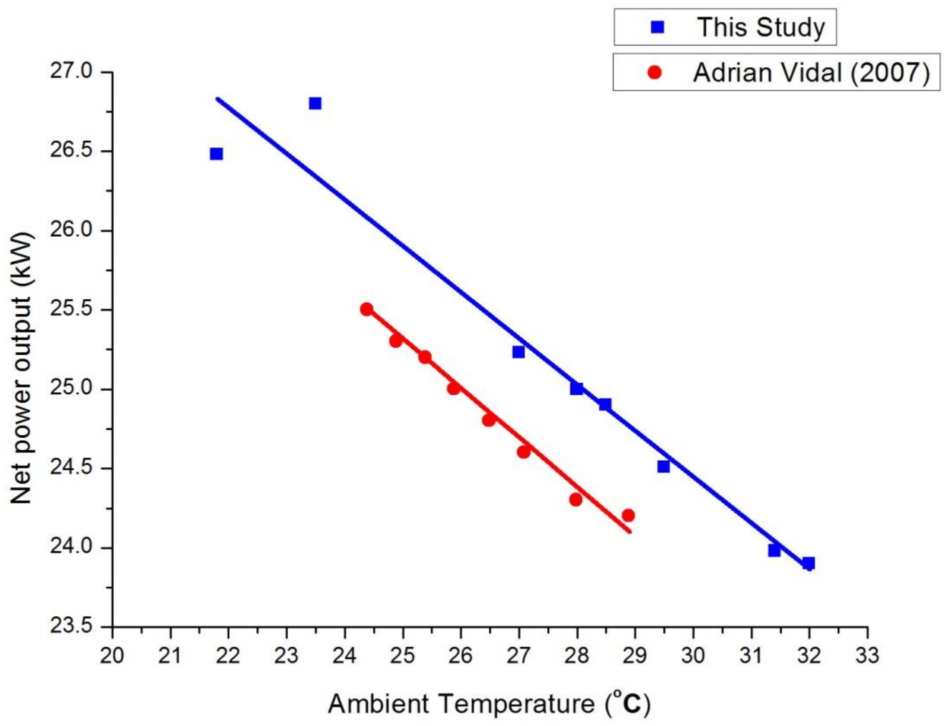

Figure 9 Least Square Method for Net Power Output

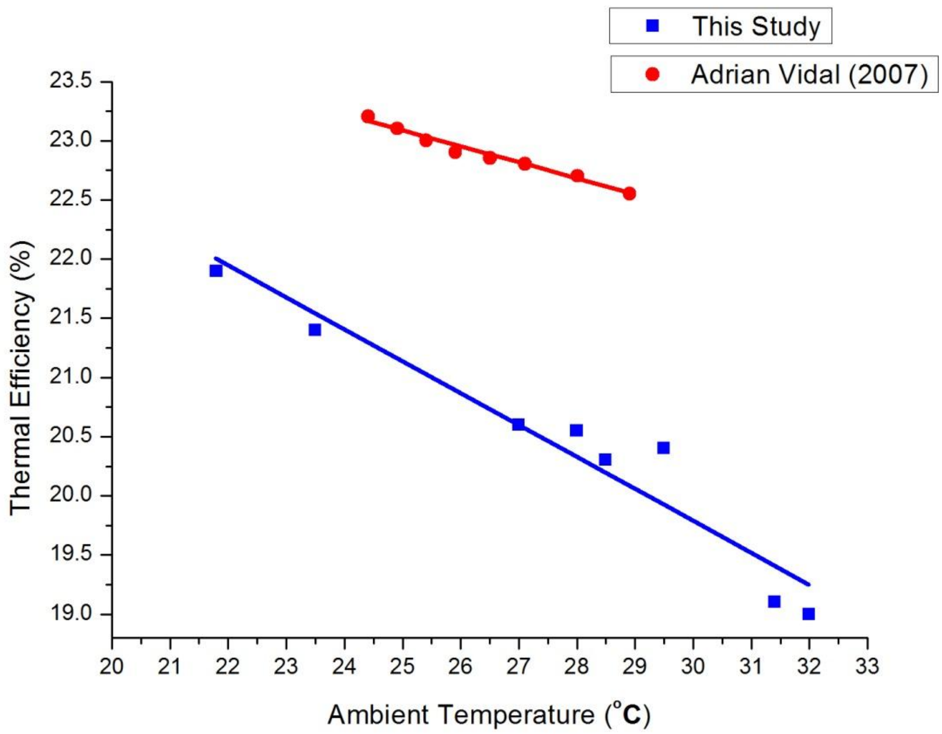

Figure 10 Least Square Method for Thermal Efficiency

VI. TALBES

Table 1 The Input Data in 25kW at 31.4°C

Constant parameters	Values
Compressor isentropic efficiency	0.767[7]
Turbine isentropic efficiency	0.83[7]
Heat exchanger effectiveness	0.786[10]
Generator efficiency	0.96[7]
Compressor mechanical efficiency	0.97[7]
Turbine mechanical efficiency	0.97[7]
Air mass flow rate	16.02 kg/min (measured)
Methane mass flow rate	0.1519 kg/min (measured)
Biogas mass flow rate	0.3478 kg/min (measured)
Hot gas mass flow rate	16.368 kg/min (measured)
Air specific heat capacity at constant pressure	1.005 kJ/kg[11]
Biogas specific heat capacity at constant pressure	2.2 kJ/kg[11]
Methane specific heat capacity at constant pressure	1.45 kJ/kg[11]
Hot gas specific heat capacity at constant pressure	1.0145 kJ/kg[11]
Pressure ratio	3.85[7]
Compressor inlet temperature	311.7 K (measured)
Turbine outlet temperature	866 K (measured)
Lower heating value of methane	50020 kJ/kg[11]

Table 2 Results of theoretical calculation

Denotation	Value
Compressor inlet temperature T_1 (measured)	302.3 K
Turbine outlet temperature T_5 (measured)	866 K
Compressor outlet temperature T_2 (calculated)	503 K
Isentropic compressor outlet temperature T_{2s} (calculated)	458 K
Heat exchanger outlet temperature T_3 (calculated)	788 K
Isentropic heat exchanger outlet temperature T_{3s} (calculated)	866 K
Combustor outlet temperature T_4 (calculated)	1185 K
Isentropic combustor outlet temperature T_{4s} (calculated)	1250 K
Isentropic turbine outlet temperature T_{5s} (calculated)	866 K
Heat exchanger outlet temperature (gas) T_6 (calculated)	581 K
Isentropic heat exchanger outlet temperature (gas) T_{6s} (calculated)	458 K
Turbine output work W_T (calculated)	85.66 kW
Compressor input work W_C (calculated)	52.82 kW
Generator power output $W_{generator}$ (calculated)	31.54 kW
Theoretical total input heat Q_{th} (calculated)	113.9 kW
Actual total input heat Q_{actual} (calculated)	126.7 kW
Theoretical thermal efficiency η_{th} (calculated)	25.62 %
Actual thermal efficiency η_{actual} (calculated)	23.04 %

Table 3 Compositions of Biogas at Inlet of Turbine Engine at different Ambient Temperature

Ambient Temperature	CH_4 (%)	CO_2 (%)	Air (%)	H_2O (%)	Residues (%)
21.8 ºC	64	19.3	10.42	1.3	4.98
23.5 ºC	51.7	20.1	25.6	1.44	1.16
29.5 ºC	60	12.73	18.37	1.44	2.36
31.4 ºC	47.8	22.3	23.13	3.17	3.6

AUTHOR INFORMATION

Corresponding Author

*Telephone: +886-3-5725634. Fax: +886-3-5728504. E-mail address: chchen@mail.nctu.edu.tw

Present Address

Department of Mechanical Engineering, National Chiao-Tung University, 1001 University Road, Hsinchu, 30056, Taiwan, R.O.C.

Notes

The authors declare no competing financial interest.

ACKNOWLEDGMENT

he authors express grateful appreciation to the National Science Council and the Ministry of Education for their financial support under the project MOST 104-3113-E-009-001. Besides, the authors are very grateful to

Aerospace Industrial Development Corporation for help in experiment and renting the micro-gas turbine engine (CR30).

REFERENCES

[1]. Tsai W. T.; Lin C. I. Overview analysis of bioenergy from livestock manure management in Taiwan. *Renew. Sust. Energ. Rev* **2009**, 13, 2682-2688.

[2]. Su J. J.; Liu B. Y.; Chang Y. C. Emission of greenhouse gas from livestock waste and wastewater treatment in Taiwan. *Agric. Ecosyst. Environ* **2003**, 95, 253-263.

[3]. Firdaus B.; Takanobu Y.; Kimio N.; Soe N. Effect of ambient temperature on the performance of micro gas turbine with cogeneration system in cold region. *Appl. Therm. Eng* **2011**, 31, 1058-1067.

[4]. Ashley D. S., Sarim A. Z. Gas turbine performance at varying ambient temperature. *Appl. Therm. Eng* **2011**, 31, 2735-2739.

[5]. Hasan H. E.; Suleyman H. S.; Effect of ambient temperature on the electricity production and fuel consumption of a simple cycle gas turbine in Turkey. *Appl. Therm. Eng* **2006**, 26, 320-326.

[6]. Naeim F.; Liu S. Qaisar Hayat. Effect of Ambient Temperature on the Performance of Gas Turbines Power Plant. *I Int. J. Comput. Sci. Issues* **2013**, 10, 439-442.

[7]. Diamantis P. B.; Anastassios G. S. Full and part load exergetic analysis of a hybrid micro gas turbine fuel cell system based on existing components. *Energy Conv. Manag.* **2012**, 64, 213-221.

[8]. Adrian V.; Joan C. B.; Roberto B.; Alberto C. Performance characteristics and modelling of a micro gas turbine for their integration with thermally activated cooling technologies. *Int. J. Energy Res*. **2007**, 119-134.

[9]. Homam N. S.; Mohammad M. M.; Peter B.; Mohsen A. Performance analysis of a biogas-fueled micro gas turbine using a validated thermodynamic model. *Appl. Therm. Eng* **2014**, 66, 181-190.

[10]. Capstone Document Library. Available: http://docs.capstoneturbine.com/login.asp.

[11]. Sonntag et al., *Fundamentals of Thermodynamics*, JOHN WILEY & SONS, INC.: New York, 1998; pp648-653.